

EXPERIMENTAL AND THEORETICAL EVALUATION OF
ELECTROMAGNETIC ENVIRONMENT PRODUCED BY
DIRECT ELECTRON INJECTION AT AURORA

M. S. Bushell, W. O. Coburn,
G. Merkel, and W. D. Scharf
US Army Electronics Research and
Development Command
HARRY DIAMOND LABORATORIES
Adelphi, MD 20783

ABSTRACT

A mosaic of experimental data accumulated during the last year or two indicates that when operated in the electron injection mode AURORA can produce a very fast electromagnetic response in a large number of sensors. These fast responses are consistent with an electromagnetic environment in the AURORA test cell that has a very fast rise time. The electromagnetic parameters that have been measured and found to have rise times less than 10ns are the electric field and the magnetic field. The rise time of the relativistic electron current has also been found to be approximately 10ns at a number of positions in the AURORA test cell, but not at all positions. Two possible mechanisms that contribute to the fast rise time are:

- 1) electric field clipping due to conductivity, and
- 2) beam erosion due to the inductance of the electron beam in the AURORA test cell.

INTRODUCTION

One of the goals of the work presented here was to obtain experimental measurements of the electromagnetic environment produced in the AURORA test cell by the direct injection of electrons. The experimental details of this procedure are discussed in references 1 and 2. Another goal was to explain the measured electric fields and magnetic fields in terms of a reasonable theoretical framework.

The work presented here is an extension of the work in reference 1, with added emphasis on the electromagnetic environment. The data now available are not sufficient to fully characterize the environment. Rather, a few more pieces of what appears to be a rather extensive mosaic will be presented.

GENERAL DISCUSSION

Figure 1 shows the dimensions of the AURORA test cell. Figure 2 shows isodose contours for a typical AURORA e-beam shot. Figure 3 compares two different E-field measurements obtained on the floor at position "X" in figure 1. The two measurements were obtained with two parallel-plate sensors--one with a plate spacing of 1/4-in. and the other 1/2-in. The two measurements were made to check the effects of radiation induced sensor noise (doubling the plate separation should double the signal induced by the E-field, but not that due to direct-drive radiation noise). This simple test suggests that the measurements are reliable. A discussion of the use of parallel-plate E-field sensors in an ionized conducting air environment is given in reference 3.

Figure 4 shows the diode current and voltage time-histories measured by Stewart Graybill (reference 1) in the AURORA coaxial tube leading to the AURORA electron emission diode. A question that immediately arises is, how can the fast electric-field rise times such as those measured on the AURORA test cell floor (figure 3) be driven by electrons that are injected by a diode with a slow acceleration voltage rise time such as that shown in figure 4?

Theoretically, if the spatial and temporal distribution of the electron current density vector, $\vec{J}(\vec{r}, t)$, and the conductivity of the ionizing air, $\sigma(\vec{r}, E, t)$, were known throughout the AURORA test cell, a finite-difference code Maxwell-equation solver could be used to calculate the response shown in figure 3. The determination and theoretical interpretation of \vec{J} and σ can be based on the thermoluminescent dosimetry (TLD) measurements described in reference 4. Of course, TLD techniques only yield information about the local integrated dose or electron current. TLD techniques yield no information about the time variation of the dose rate during the deposition of the total dose. Nor is any information on the directionality of the particles available from such data. As a first order approximation, the dose-rate waveform can be assumed to be the same throughout the entire test cell (varying only in amplitude). But more success has been achieved using a more complicated scheme.

The most successful approach to the interpretation of the experimental results has been to assume that the value \vec{J} can be approximated by the sum of two products such as

$$\vec{J}(t, \vec{r}) = T_1(t)\vec{R}_1(\vec{r}) + T_2(t)\vec{R}_2(\vec{r}) . \quad (1)$$

Figure 5 compares a finite-difference calculation using the THREDE⁵ code (assuming current drivers of the form shown in equation (1)), and experimental results. Calculations using drivers of the form shown in equation (1) yield E-fields that have the experimentally measured shape and magnitude over most of the test volume. As will be explained in a later section of the paper, distributions of the type shown in equation (1) are needed to incorporate the complicated temporal and spatial variation of the electrons. The early and late parts of the injected e-beam correspond to low-energy electrons that have ranges shorter than the AURORA test cell. These low-energy electrons can result in the deposition of an appreciable amount of charge into the volume of the test cell. The high-energy portion of the energy distribution of the injected electrons corresponds to electron ranges which terminate in

Report Documentation Page				Form Approved OMB No. 0704-0188	
Public reporting burden for the collection of information is estimated to average 1 hour per response, including the time for reviewing instructions, searching existing data sources, gathering and maintaining the data needed, and completing and reviewing the collection of information. Send comments regarding this burden estimate or any other aspect of this collection of information, including suggestions for reducing this burden, to Washington Headquarters Services, Directorate for Information Operations and Reports, 1215 Jefferson Davis Highway, Suite 1204, Arlington VA 22202-4302. Respondents should be aware that notwithstanding any other provision of law, no person shall be subject to a penalty for failing to comply with a collection of information if it does not display a currently valid OMB control number.					
1. REPORT DATE JUN 1983		2. REPORT TYPE N/A		3. DATES COVERED -	
4. TITLE AND SUBTITLE Experimental And Theoretical Evaluation Of Electromagnetic Environment Produced By Direct Electron Injection At Aurora				5a. CONTRACT NUMBER	
				5b. GRANT NUMBER	
				5c. PROGRAM ELEMENT NUMBER	
6. AUTHOR(S)				5d. PROJECT NUMBER	
				5e. TASK NUMBER	
				5f. WORK UNIT NUMBER	
7. PERFORMING ORGANIZATION NAME(S) AND ADDRESS(ES) US Army Electronics Research and Development Command HARRY DIAMOND LABORATORIES Adelphi, MD 20783				8. PERFORMING ORGANIZATION REPORT NUMBER	
9. SPONSORING/MONITORING AGENCY NAME(S) AND ADDRESS(ES)				10. SPONSOR/MONITOR'S ACRONYM(S)	
				11. SPONSOR/MONITOR'S REPORT NUMBER(S)	
12. DISTRIBUTION/AVAILABILITY STATEMENT Approved for public release, distribution unlimited					
13. SUPPLEMENTARY NOTES See also ADM002371. 2013 IEEE Pulsed Power Conference, Digest of Technical Papers 1976-2013, and Abstracts of the 2013 IEEE International Conference on Plasma Science. Held in San Francisco, CA on 16-21 June 2013. U.S. Government or Federal Purpose Rights License					
14. ABSTRACT A mosaic of experimental data accumulated during the last year or two indicates that when operated in the electron injection mode AURORA can produce a very fast electromagnetic response in a large number of sensors. These fast responses are consistent with an electromagnetic environment in the AURORA test cell that has a very fast rise time. The electromagnetic parameters that have been measured and found to have rise times less than 10ns are the electric field and the magnetic field. The rise time of the relativistic electron current has also been found to be approximately 10ns at a number of positions in the AURORA test cell, but not at all positions. Two possible mechanisms that contribute to the fast rise time are: 1) electric field clipping due to conductivity, and 2) beam erosion due to the inductance of the electron beam in the AURORA test cell.					
15. SUBJECT TERMS					
16. SECURITY CLASSIFICATION OF:			17. LIMITATION OF ABSTRACT SAR	18. NUMBER OF PAGES 4	19a. NAME OF RESPONSIBLE PERSON
a. REPORT unclassified	b. ABSTRACT unclassified	c. THIS PAGE unclassified			

the conducting walls of the AURORA test cell.

The results obtained with a large, complicated finite difference code are frequently difficult to interpret. These codes include a great number of phenomena whose relative importance is difficult to determine. A number of simple models and arguments can, however, yield insight into the general shape of the measured E-field and the necessity of using an expression of the form (1) for the current driver.

CLIPPING

One of the factors contributing to the fast rise-time of the E-field pulse is the clipping effect of air conductivity. Consider Maxwell's equation for the curl of H:

$$\nabla \times H = \epsilon_0 \frac{dE}{dt} + \sigma(t, E)E + J \quad (2)$$

where J is the electron current density produced by the electrons injected into the AURORA test cell. In a region in the center of the AURORA test cell, far from the walls, $\nabla \times H = 0$, and equation (2) becomes

$$\epsilon_0 \frac{dE}{dt} + \sigma(t, E)E + J = 0 \quad (3)$$

The solution to this purely local (no spatial derivatives) equation for a number of different electron current densities, but with the same rise time, is shown in figure 6. Figure 7 shows an equivalent circuit that is an analog to equation (3). The shape of the curves in figure 6 can be explained in terms of a clipping or limiting action of the time-varying resistance across the capacitor in figure 7. It is easy to see from this analysis how even a slowly rising electron current density can produce an electric field with a fast rise time.

BEAM INDUCTANCE

A number of electron current density measurements have also been made (see reference 6). The results of two of these measurements are shown in figures 8 and 9. As can be seen, there is a rise-time enhancement as the electron beam propagates along the AURORA test cell. Figure 10 shows a magnetic-field measurement obtained on the floor at position "Y" in figure 1 with a large loop. This measurement implies a very fast build up of total current, (i.e., $J_{total} = \sigma E + J$) in the AURORA test cell. A good candidate for the cause of the shortened rise time of the injected e-beam is beam inductance. Let I_b be the total beam current injected into the AURORA test cell, and let I_r be the return current in the beam channel. Then the net current, I_{net} , will be

$$I_{net} = I_{beam} - I_{return}$$

Figure 11a is a schematic diagram that shows these currents in the AURORA test cell. Consider the simplest geometry, i.e., a homogeneous beam with net current I_{net} and radius R_b propagating down a pipe with radius R_w . Then the value of the electric field that opposes the increase in e-beam current is

$$E_z = \frac{\mu_0 \dot{I}_{net}}{2\pi} \left(\frac{1}{2} + \ln \frac{R_w}{R_b} \right) \approx \frac{\mu_0 \dot{I}_{net}}{4\pi} \quad .$$

Note that at the beginning of the beam current pulse, the energy of the electrons is small and the opposing field E_z will have its greatest effect.

Figure 11a shows a loop antenna positioned to yield information about the value of I_{net} . The magnetic field measurement shown in figure 10 implies an I_{net} of approximately 40 kA; this is to be compared to an I_{beam} of approximately 250 kA. The rise time of the loop response is approximately $\Delta t = 10^{-8}$ seconds, therefore,

$$E_z = 4 \times 10^5 = 400 \text{ kV/m} \quad .$$

Figure 11b shows the results of a 3-dimensional finite difference code calculation of the electric field E_z . The magnitude of the code prediction compares favorably with the value of 400 kV/m just calculated.

The dip in the pulse takes place at maximum e-beam current and is the result of the large air conductivity produced by the large number of secondary conduction electrons concomitant with the large beam current.

QUASI-STATIC CHARGE RELAXATION

As the beam pulse of injected electrons comes to an end, two things occur: the energy of the injected electrons decreases and the magnitude of the beam current also decreases. At the peak of the electron emission pulse the AURORA diode voltage and the e-beam current are both relatively slowly varying, and the injected electrons have long trajectories that terminate in the metallic walls of the cell. However, as the AURORA diode voltage decreases, the energy of accelerated electrons also decreases and the electrons that are injected into the AURORA test cell have trajectories that terminate in the volume of the cell. The shorter electron trajectories are accompanied by decreasing beam currents and hence decreasing ionized air conductivities. (The conduction electrons that are lost due to oxygen molecule attachment are only partially replenished by secondary electrons produced by the beam current.) The result of the short-range electrons and diminished air conductivity is a large increase in the E-field in the AURORA test cell produced by trapped charge. The trapped charge eventually leaks out of the AURORA test cell, and the slow decay of the late-time E-field pulse is consistent with the low value of air conductivity characterized by heavy-ion carriers.

The decay of the second pulse in the E-field can be discussed in terms of the conservation of charge and Gauss's law. It is easy to show that the decay of the E-field is given by

$$E = E_0(t/t_0)^{-\mu_I \epsilon / \epsilon k}$$

where k is the ionic recombination constant and μ_I the average ionic mobility.

CONCLUSION

To recapitulate: (1) beam erosion (caused by the large inductive E-field) plus air conductivity clipping produce an E-field in the AURORA test cell with a rise time in the nanosecond regime, (2) the large air conductivity at maximum beam current shorts out the E-field

in the AURORA test cell, and (3) after the AURORA pulse terminates, there is a large quasi-static E-field, produced by trapped charge, that is slowly neutralized by virtue of ionic air conductivity.

REFERENCES

1. S. E. Graybill, "AURORA Electron Beam Modifications," HDL-TR-1862, July 1978.
2. M. Bushell, S. E. Graybill, K. G. Kerris, G. Merkel, W. D. Scharf, and D. A. Whittaker, "The Direct Injection of Electron Pulses into Air--A SREMP Simulation Tool," 3rd IEEE International Pulsed Power Conference, Albuquerque, New Mexico, June 1981.
3. M. Bushell, R. Manriquez, G. Merkel, and W. D. Scharf, "Simulated Coupling To Cylindrical Objects," IEEE Trans. Nucl. Sci. NS-28, No. 6, December 1981.
4. R. P. Manriquez, G. Merkel, W. D. Scharf, and D. J. Spohn, "Electrically Short Monopole Antenna Response in an Ionized Air Environment--Determination of Ionized Air Conductivity," IEEE Trans. Nucl. Sci. NS-26, No. 6, December 1979.
5. Klaus Kerris, "The AURORA Dosimetry System," HDL-TR-1754, March 1976.
6. M. Bushell, R. Manriquez, G. Merkel and W. D. Scharf, "Electronic Response of Long Cylindrical Structures and Large Loops in an Inhomogeneous Medium With Time-Varying Conductivity," IEEE Trans. Nucl. Sci. NS-29, No. 6, December 1982.
7. C. L. Longmire, G. Merkel and D. J. Spohn, "Simple Compton Current Density Measurement Technique," IEEE Trans. Nucl. Sci. NS-24, No. 6, December 1977.

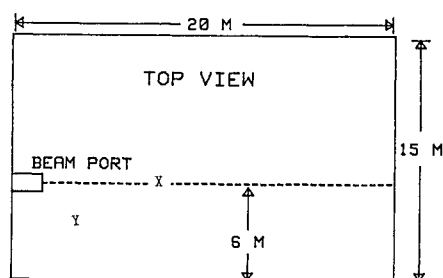


Figure 1. Top view of AURORA test cell.

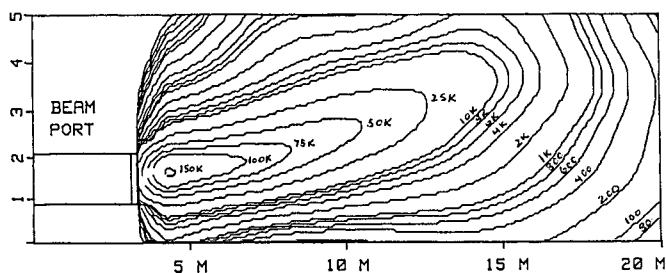


Figure 2. Side view of AURORA test cell showing isodose contours for typical electron beam shot. Doses are in rads(silicon). From dosimetry data taken by Klaus Kerris.

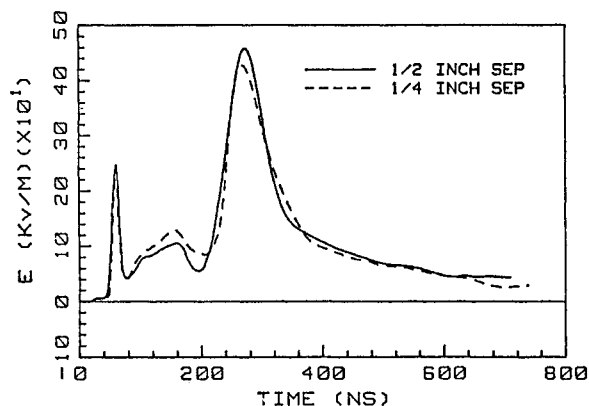


Figure 3. Comparison between electric field measurements made with a 12 inch wire grid sensor with different plate separations.

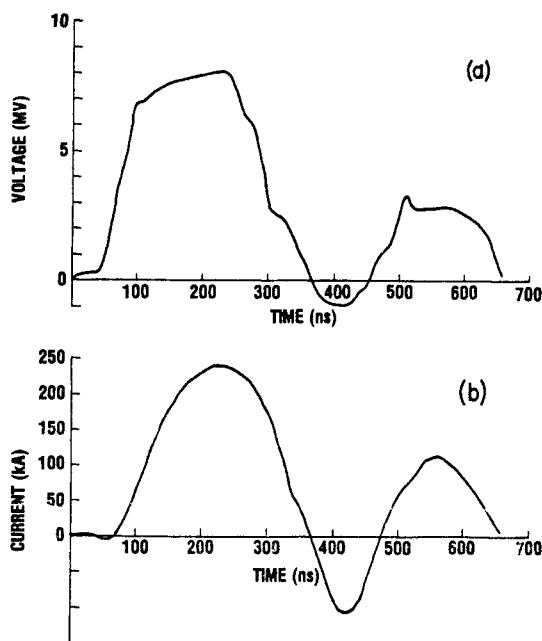


Figure 4. AURORA cathode voltage (a) and cathode current (b) as a function of time for a 90-KV charging voltage. From Ref. 1.

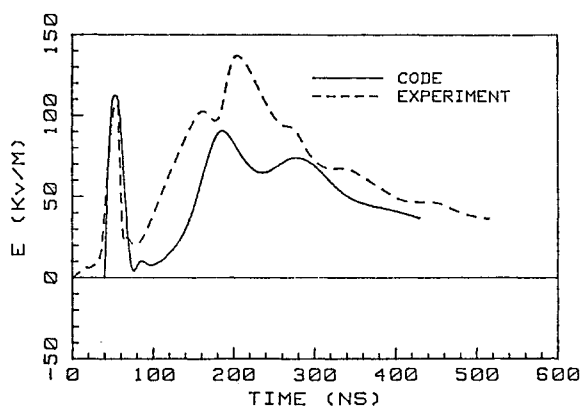


Figure 5. Comparison between experimental measurement and HDL SREMP Group finite-difference code prediction of electric field in AURORA test cell at 10 meter mark during e-beam test (Shot number 3957)

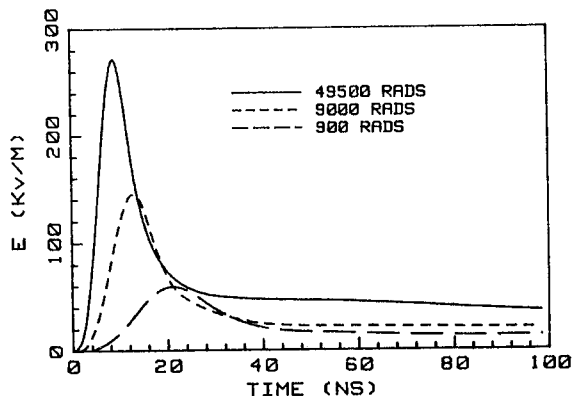


Figure 6. Solution of equation 3 for various peak dose rates. The driving radiation pulse, which was the same in each case except for a multiplicative scale factor, peaked at about 40 ns (well after all the E-field peaks).

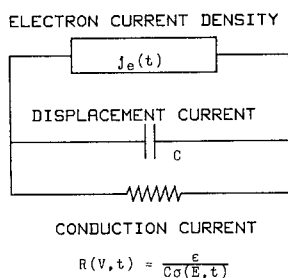


Figure 7. Equivalent circuit yielding results consistent with curves shown in figures 5 and 7.

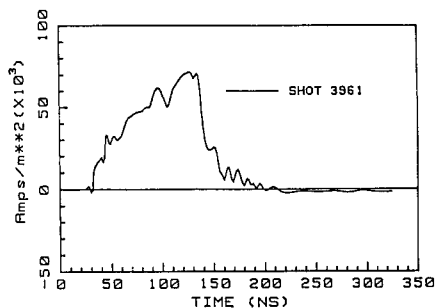


Figure 8. Compton current measurement made in AURORA on beam center line at 5.62 meter mark 1.5 meters off floor during e-beam test.

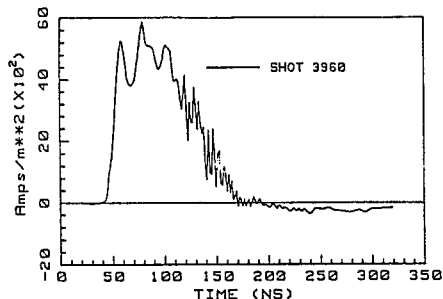


Figure 9. Compton current measurement made in AURORA on beam center line at 8.75 meter mark 1 meter off floor during e-beam test.

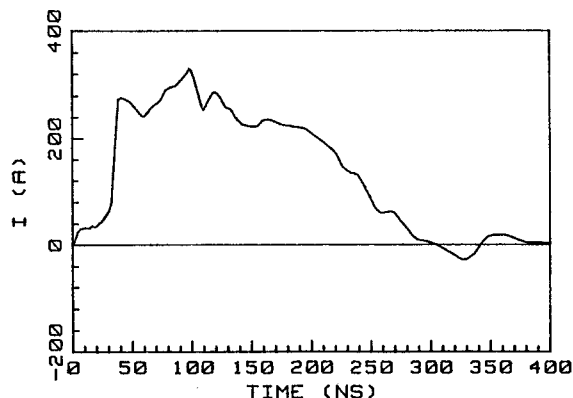


Figure 10. Current response of self-integrating magnetic field loop positioned in AURORA test cell as shown in Fig. 11a.

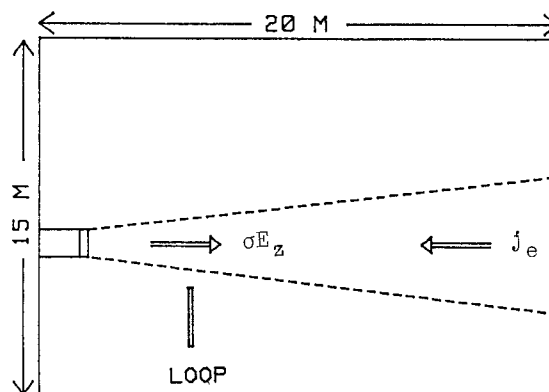


Figure 11a. Schematic drawing of AURORA test cell. The electron current density, j_e , is injected into the test cell. The inductive electric field, E_z , causes a current density σE_z , to flow in the opposite direction. The magnetic field loop placed as shown responds to the total current density, $j_{tot} = j_e + \sigma E_z$.

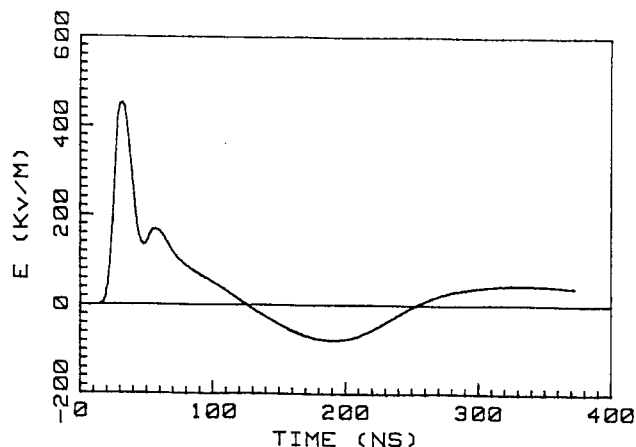


Figure 11b. Finite-difference code prediction of forward E-field at beam center 3 meters from snout. The direction of this field is such that at early times it opposes the propagation of the electrons in the beam.